ISET Journal of Earthquake Technology, Paper No. 592, Vol. 62, No. 1, March 2025, pp. 35-46

FREQUENT MODERATE EARTHQUAKES IN THE VICINITY OF THE KULSI FAULT: IMPLICATIONS FOR FUTURE LARGE EVENTS

William Kumar Mohanty (Corresponding Author)
Professor, Department of Geology and Geophysics
Indian Institute of Technology Kharagpur, 721302, India, E mail id: wkmohanty@gg.iitkgp.ac.in

Mohd Shahabuddin
Research Scholar, Department of Geology and Geophysics
Indian Institute of Technology Kharagpur, 721302, India, E mail id: mohdshahabuddin@iitkgp.ac.in

Suvankar Samantaray
Research Scholar, Department of Geology and Geophysics
Indian Institute of Technology Kharagpur, 721302, India, E mail id: samantarayshuvankar@gmail.com

Priyank Pathak
Research Scholar, Department of Geology and Geophysics
Indian Institute of Technology Kharagpur, 721302, India, E mail id: priyank.pathak.125@gmail.com

ABSTRACT

The Shillong Plateau and Northeast India constitute a seismically active region, influenced by the Himalayan orogeny and the ongoing collision between the Indian and Eurasian plates. This study focuses on the seismicity of the Shillong Plateau, with particular emphasis on recent earthquakes occurring along previously inactive faults, such as the Kulsi Fault. The objective is to understand the implications for future large seismic events. An earthquake catalog compiled for the period 815–2022, containing 2,966 events, has been analyzed. Notably, a recent earthquake of magnitude m_b 4.3 occurred in the West Khasi Hills district of Meghalaya, India, on July 16, 2023. Within a 100 km radius of the Kulsi Fault, 40, 108, and 56 earthquakes of magnitude ranges 4.0–5.0, 3.0–3.9, and 2.0–2.9, respectively, have been recorded over the past decade. Additionally, the region has experienced six major earthquakes of magnitude greater than 6.0. The magnitude of completeness (M_c) for the catalog is estimated at 3.0, with spatial variations ranging from 2.7 to 3.8. The calculated b-value and a-value for the entire study area are 0.62 ± 0.04 and 4.8, respectively. Spatial mapping of the b-value indicates that the northeastern segment of the Kulsi Fault is more highly stressed compared to its northwestern counterpart. Return periods for an earthquake of magnitude 5.8 have been estimated for each of the four seismic zones delineated. Furthermore, a strike-slip nature for the Kulsi Fault has been identified based on terrestrial gravity data, with Bouguer anomaly variations ranging from 32.05 to 8.40 mGal across the fault. Deflected Bouguer anomaly contours along the fault line further corroborate its existence. The increased frequency of earthquakes in recent years, particularly in the central portion of the Shillong Plateau, suggests the emergence of a new hub of seismic activity. These findings provide critical insights for seismic hazard assessment and risk mitigation in the region.

KEYWORDS: Kulsi Fault, Shillong Plateau, Seismicity, B-Value, Bouguer Anomaly

INTRODUCTION

The northward-moving Indian plate has led to its oblique collision with the Eurasian plate in the north and the Burmese plate in the east, forming the Himalayas in the north and the Indo-Burmese ranges in the east, respectively. Flanked by these two active mountain belts, northeast India represents one of the most seismically active regions of the Indian subcontinent and lies in seismic zone V, the highest hazard according to the seismic zoning map of India (BIS 2002). The Shillong Plateau (SP) is a unique tectonic feature within northeast India, characterized by a pop-up structure bounded by two major reverse faults dipping towards each other, resulting in significant tectonic uplift. SP has experienced many major to great earthquakes in past, such as 825, M = 8; 1787, M = 7.8; 1869 Cachar earthquake, M_w = 7.5; 1897 Assam earthquake, M = 8.1; 1923 Meghalaya earthquake, Mw =7.1; 1930

https://doi.org/10.63898/PPRT5903

Dhubri earthquake, M_s =7.1; 1943 Assam earthquake, M_s = 7.1; 1950 Assam earthquake, M_w = 8.7; 1954, M = 7.3 etc. (Oldham 1882, 1899; Iyengar et al. 1999; CNDM 2002; Rajendran et al. 2004). A number of studies have been performed by various researchers to examine the seismicity of northeast India using various techniques due to its active, prolonged seismic history and complex tectonics (Bhattacharya et al. 2002; Khan 2005; Thingbaijam et al. 2008; Yadav et al. 2009, 2023; Khan et al. 2011; Pandey et al. 2017, 2019; Borgohain et al. 2018a, b; Bora et al. 2022; Sharma et al. 2022; Sharma and Biswas 2022; Kumar et al. 2024). Previous researchers have considered different statistical methods to quantify the seismicity of the region; however, very few studies are focused on the Shillong plateau. Bhattacharya et al. (2002) estimated the b-value and fractal dimension of northeast India using very limited earthquake data from the International Seismological Center (ISC), National Geophysical Research Institute (NGRI), Hyderabad, and the Regional Research Laboratory Jorhat (RRLJ). Khan (2005) mapped b-value using earthquake data from only the NGRI, Hyderabad, and RRLJ, and estimated the Bouguer gravity anomaly to examine the seismicity of the Shillong plateau. Thingbaijam et al. (2008) estimated seismicity parameters and fractal dimension of northeast India using earthquake data of ISC and Global Centroid Moment Tensor (GCMT) for the period 1906 to 2006. Yadav et al. (2023) estimated the b-value and fractal dimension of northeast India using earthquake data of ISC, GCMT, India Meteorological Department (IMD), and United States Geological Survey (USGS) for the period 1897 to 2016. Pandey (2019) estimated the b value of the northeast India using earthquake data of ISC and GCMT for the period 1963 to 2012. Borgohain et al. (2018a) examined the seismicity of the SP using earthquake data of ISC, USGS, RRLJ, and NGRI for the period 1966 to 2013. Bora et al. (2018) and Bora et al. (2022) estimated the b-value of the Indo Burman Range using earthquake data of ISC for the period 1964 to 2016 and 1964 to 2018, respectively. Sharma et al. (2022) performed a Spatio-temporal analysis of the b-value prior to the 28 April 2021 Assam earthquake. Kumar et al. (2024) estimated the spatial variation of seismicity parameters in Meghalaya. Sharma and Biswas (2024) estimated the seismic hazard and delineated the seismic sources around the Kopili fault. Relatively fewer studies have been specifically focused on the Shillong Plateau using updated datasets and high-resolution analyses. Earlier works, though insightful, often relied on limited earthquake records (from ISC, NGRI, RRLJ) and did not integrate modern seismic catalogues, gravity anomaly data, or recent earthquake activity around emerging structures like the Kulsi Fault. In recent years, the Shillong Plateau has witnessed rapid urbanization, population growth (~30 million), and the development of critical infrastructure, significantly increasing the seismic risk exposure. The recurrence of moderate earthquakes around the Kulsi Fault, including the recent 16 July 2023 m_b 4.2 event, further emphasizes the need for a dedicated and updated seismic hazard assessment. In addition, Verma and Mukhopadhyay (1977) collected the gravity data in northeast India, and they found a high positive Bouguer anomaly over the Shillong Plateau and suggested that it may be due to high irregularities in the crustal and mantle structures. Afterwards, a different group of scientists has also reported a higher Bouguer anomaly over the Shillong Plateau than its adjoining regions, and they argued that it is due to high magmatic material beneath it as well as its pop-up basement (e.g., Nayak et al., 2008; Ravi Kumar et al., 2020; Sarkar et al., 2022).

In the present study, we analyze the current seismicity, tectonic framework, and earthquake occurrence potential of the Shillong plateau and adjoining region, focusing particularly on the area within 100 km of the recently occurred 16 July 2023 Kulsi earthquake (m_b 4.2). and estimated the seismicity parameters of the study region as a continuous increase in the occurrence of earthquakes near the Kulsi fault. In addition, we delineate seismic source zones based on updated seismicity and tectonic information and estimated seismic hazard parameters for each zone. Furthermore, we also identify the major faults from the gravity anomaly map and establish the relationship between the seismicity and active faults (both exposed and blind faults).

DATA AND METHODS

In the present study, we considered a region within 100 Km of the epicenter of the m_b 4.2 Kulsi fault earthquake, which is bounded by 24.5°N-26.5°N latitude and 90.5°E-92.5°E longitude, as shown in Figure 1. Two different data sets, like earthquake data and gravity data, have been used. We have compiled an earthquake catalogue from various national and international agencies, as well as literature,

covering the period from 815 to 2022. Gravity data have been obtained by field surveys using a Worden gravimeter.

SEISMICITY ANALYSIS

1. Homogeneous Earthquake Catalogue

An earthquake catalogue compiled by Shahabuddin and Mohanty (2025) is used in the present study. It incorporates data from multiple national and international agencies, including the ISC, GCMT, and NCS, as well as various published sources. Duplicate events have been removed manually. The earthquake magnitudes are heterogeneous, as different agencies report using different magnitude scales (Richter 1935; Cornell 1968; Hanks and Kanamori 1979; Choy and Boatwright 1995). Many of these magnitude scales are known to saturate at higher magnitudes, except for moment magnitude (M_W) (Richter 1935; Kanamori 1983; Lay and Wallace 1995). All reported magnitudes are homogenized to moment magnitude (M_W) using regression relations developed between various magnitude scales by Shahabuddin and Mohanty (2025). The compiled earthquake catalogue contains 2,966 earthquakes for the period of 815-2022. Hypocenter depth of the majority of earthquakes lies between 10 and 45 Km Figure 2).

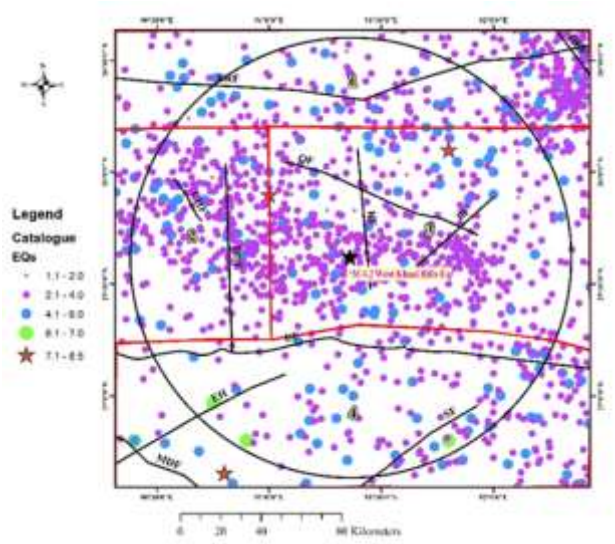

Fig. 1 Seismicity of the SP and adjoining region and M 4.2 Kulsi fault earthquake (black star). BF: Barapani fault, BRF: Brahmputra Fault, CHF: Churachandpur Fault, DF: Dauki Fault, DDF: Dudhnoi Fault, EH: Eocene Hinge, KF: Kulsi Fault, MDF: Madhubani Fault, OF: Oldham Fault, SF: Sylhet Fault.

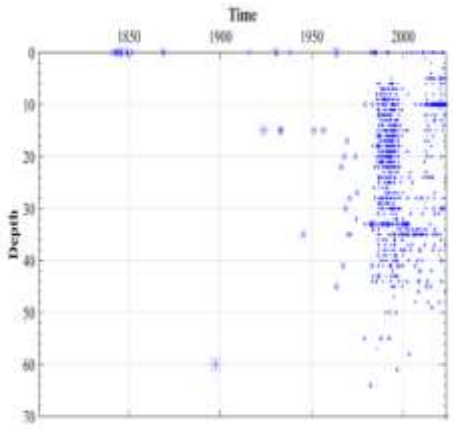

Fig. 2 Hypocentral distribution of the compiled earthquake catalogue.

2. Seismic Source Zonation

The study region is divided into four seismic source zones based on the seismicity and tectonics of the area, as shown in Figure 1. Zone 1 comprises the Brahmaputra Fault (BRF) and includes 233 earthquakes, with a maximum magnitude of 5.8, located north of the Shillong Plateau. Zone 2 comprises the Churachandpur Fault (CHF) and the Dudhnoi Fault (DDF), with a maximum magnitude earthquake of 8.1. A total of 143 earthquakes have occurred in Zone 2. Zone 3 includes the Kopili Fault (KF), Oldham Fault (OF), and Barapani Fault (BF), along with the M 4.2 West Khasi Hills earthquake. This zone has experienced 397 earthquakes, including a maximum observed magnitude of 8.1. Zone 4 comprises the Dauki Fault (DF), Sylhet Fault (SF), Eocene Hinge (EH) tectonic region, and Madhubani Fault (MDF), located south of the Shillong Plateau. A total of 200 earthquakes have occurred in this zone, with a maximum magnitude of 7.2.

The delineated seismic source zones are validated through a comprehensive approach to ensure their geological, tectonic, and seismological consistency. First, the source boundaries are cross-verified against the regional tectonic framework, active fault maps, and gravity anomaly data to confirm alignment with known geological structures and major fault systems. Second, the historical and instrumental earthquake distributions are superimposed onto the defined zones to assess whether seismic activity clusters correspond logically to the zonation. Third, seismicity parameters, including the b-value and magnitude of completeness (M_C), are computed separately for each source zone to verify internal homogeneity; significant variability within a zone would indicate the need for further subdivision. Fourth, available focal mechanism solutions were reviewed to ensure that each zone exhibits relatively consistent styles of faulting appropriate to the tectonic setting. Fifth, the delineated zones are compared with previous seismic source models developed for the region (e.g., BIS, 2002; Bhatia et al., 1999) to ensure consistency while incorporating updated knowledge and higher-resolution data. Through this multi-criteria validation process, we ensured that the defined seismic source zones provide a robust basis for reliable estimation of seismic hazard parameters.

3. Magnitude of Completeness

We utilized the maximum curvature technique aided with bootstrapping and a correction factor of $M_C = M_C\,(MAXC) + 0.2$ as proposed by Woessner and Wiemer (2005) for the estimation of M_C using ZMAP software (Wiemer and Wyss 2000; Wiemer 2001; Schorlemmer et al. 2003; Woessner and Wiemer 2005). M_C is estimated at each node of a 0.5×0.5 Km grid. The spatial distribution map of estimated M_C values is generated by plotting the calculated values at each grid node using ArcGIS.

4. b-Value Estimation

We used the maximum likelihood method, proposed by Aki (1965) and corrected by Utsu (1965), commonly known as the Aki-Utsu maximum likelihood method, for the estimation of the b-value for the study region. The formula suggested is given as (Aki 1965; Utsu 1965),

$$b = \frac{\log_e 10}{\overline{M} - \left(M_C - \frac{\Delta M_{bin}}{2}\right)} \tag{1}$$

Where $\overline{M}$ is the average magnitude, M_{bin} is the magnitude bin. Standard deviation of b-value, δb, can be estimated using Shi and Bolt (1982) formula given as (Shi and Bolt 1982):

$$\delta b = 2.30 \quad (b^2) \quad \sqrt[2]{\sum_{i=1}^{n} \frac{M_i - \overline{M}}{n(n-1)}} \tag{2}$$

b-values are estimated at each node of a 0.5×0.5 Km grid, taking a minimum of 50 events at each node and 100 bootstraps. The spatial distribution map of estimated b-values is generated by plotting the calculated values at each grid node using ArcGIS.

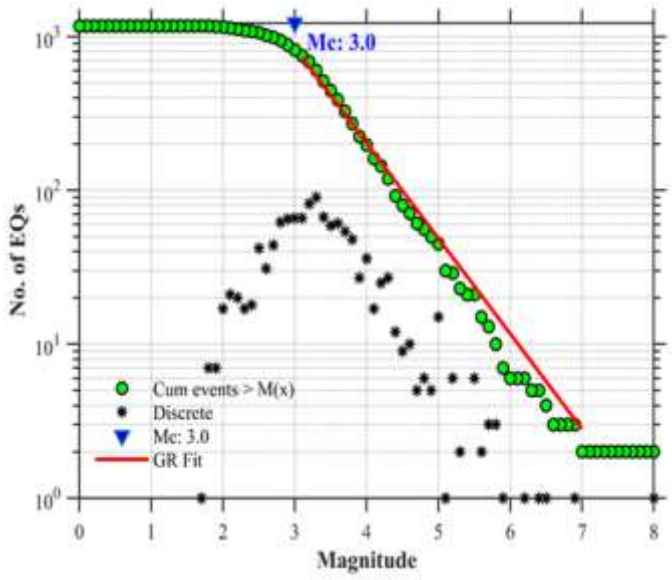

Fig. 3 M_W derived frequency-magnitude distribution. A straight line is the best fit using the G-R relationship.

ESTIMATION OF SOURCE PARAMETERS

Source parameters of each seismic source are estimated. We used Kijko–Sellevoll–Bayes (K-S-B) method to estimate the maximum magnitude of each zone, Table 1 (Kijko 2004). Return period of earthquakes of magnitude greater than M 5.8 is also estimated and listed in Table 1.

Table 1: Seismicity parameters of each zone

Zones	M_{max} obs	No of EQs	M_{max} K-S-B	RP (Years) (M 5.8)
Zone 1	5.8	233	5.90 ±0.26	52.5
Zone 2	8.1	243	8.60 ±0.33	13.4
Zone 3	8.1	397	8.32 ±0.33	17.3
Zone 4	7.2	200	7.29 ±0.31	13.3

GRAVITY DATA ANALYSIS

1. Gravity Data Acquisition

We have conducted field surveys to obtain the gravity data of the study regions. We used the Worden gravimeter, which has a sensitivity of 0.01 mGal ($1mGal=10^{-5}m/s^2$), to obtain the gravity values. A total of 203 gravity observations are measured over the study area along one east-west profile (108 observations) and one north-south profile (95 observations) with a station interval of 2.5 km, as shown in Figure 4. The gravity measurements obtained from the study area are tied to the nearest absolute gravity base station at the Jorhat engineering college (Absolute gravity value (g_n) = 978885.4 mGal). Station locations (latitude and longitude) and elevations are obtained by using differential global positioning system (DGPS).

2. Gravity Data Processing

A gravity survey involves certain uncertainties, including instrument error, which limits the ability to detect variations smaller than the sensitivity of the instrument, as well as drift correction, tidal

correction, latitude correction, topographic (free air and Bouguer correction), and terrain corrections. Tidal variations are generally very small, often below the instrument's sensitivity, and are sometimes neglected for this reason. It was processed to calculate the free air and Bouguer anomaly by correcting for instrument drift, then latitude correction, followed by free air and Bouguer correction.

All the raw gravity data are processed to reduce them to the datum plane value. First, we account for instrumental drift by occupying the base station twice, once at the beginning and again at the end of each working day. The instrument drift is estimated by dividing the gravity reading difference by the time difference between the beginning and end of the survey. It is estimated to correct the instrument drift caused by temperature. Corrected readings are obtained at each station by subtracting the drift from each station's measurements. Free-air and Bouguer corrections are then applied to isolate the subsurface density distribution. The theoretical gravity value is calculated using the 1967 Geodetic Reference System (GRS67). The free-air correction is derived using the standard free-air gradient of 0.3086 mGal/m (neglecting higher-order terms). To compute the Bouguer correction, an average crustal density of 2670 kg/m^3 is used. In addition to removing the gravity effect due to hilly and undulatory terrain, which surrounds gravity stations, a correction was applied using the recent ultrahigh resolution terrain gravity correction model, SRTM2gravity (Hirt et al., 2019).

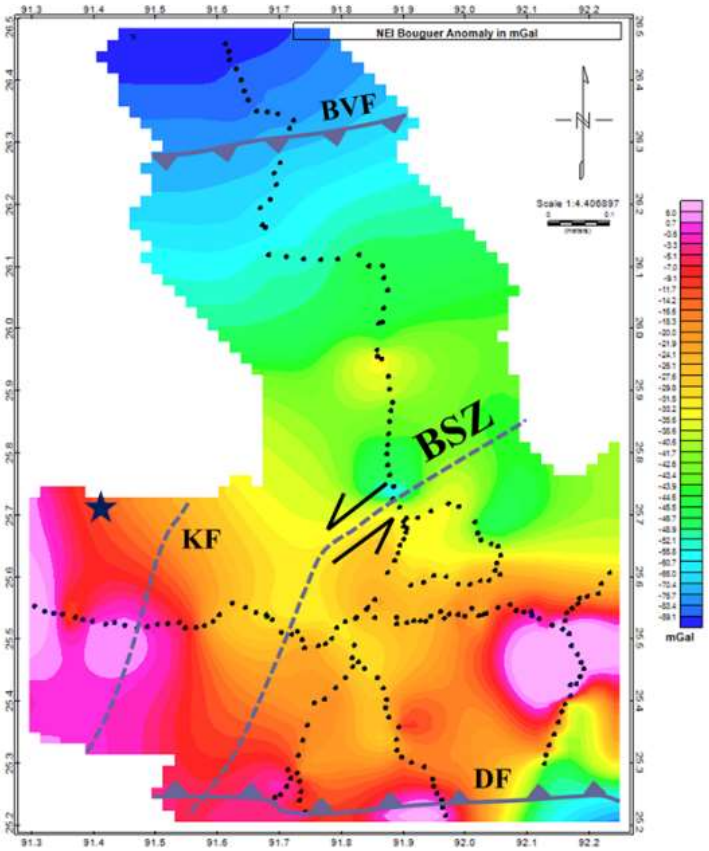

Fig. 4 Bouguer anomaly map of the study area. The black dots are the gravity station points. KF- Kulsi Fault, DF- Dauki Fault, BVF- Brahmaputra Valley Fault, BSZ- Barapani Shear Zone. The black star mark is the July 2023 earthquake epicenter.

RESULTS AND DISCUSSION

We considered the study region within a 100 km radius centered on the epicenter of the recently occurred West Khasi Hills earthquake, which had a magnitude of 4.2. The homogenized and compiled earthquake catalogue consists primarily of shallow crustal earthquakes (10–40 km) (Figure 2). The Gutenberg-Richter Frequency-Magnitude power law fit results show an average magnitude of completeness (M_C) of 3.0, with a mean b-value of 0.62±0.04 and an a-value of 4.8 (Figure 3). As the b-

value is inversely related to regional stress (Scholz 1968; Wyss 1973; Urbancic et al. 1992; Wyss et al. 1997), this lower mean b-value indicates that the region is highly stressed. The spatial distribution of M_C ranges from 2.7 to 3.8, estimated at each node of a grid with 0.5×0.5 km intervals, considering a minimum of 50 events nearest to the grid center and applying a bootstrap of 100 iterations (Figure 5). Around the epicenter of the West Khasi Hills earthquake, the M_C ranges from 2.7 to 3.0. To the northeast of the epicenter, M_C ranges from 3.30 to 3.40, while in the surrounding areas closer to the epicenter, it varies between 2.70 and 3.20. To the northwest and south of the epicenter, M_C ranges from 3.50 to 3.60. The b-value of the region is estimated by considering earthquakes with magnitudes above 3.0 (M_C), i.e., using only the complete catalogue, and applying the maximum likelihood method. The spatial distribution of b-values shows variation from 0.49 to 1.06. The b-value at the epicenter of the West Khasi Hills earthquake ranges from 0.59 to 0.67, while in the northern area of the epicenter, it ranges from 0.49 to 0.59, and in the eastern and western sides, it ranges from 0.67 to 0.75. The spatial distribution of b-values shows that the epicentral region of the West Khasi Hills earthquake is highly stressed as compared to the outer regions, as shown in Figure 6. The a-value indicates seismic activity of the region, and its spatial distribution shows that it ranges from 3.44 to 5.34. We delineated four seismic source zones based on seismotectonics (Figure 1) and estimated M_{max} and return period for zone 1, zone 2, zone 3, and zone 4 (Figure 7 and Table 1). The estimated M_{max} values are 5.90±0.26, 8.60±0.33, 8.32±0.33, and 7.29±0.31 for zone 1, zone 2, zone 3, and zone 4, respectively. The return periods of an earthquake M=5.8 are 52.5 years for zone 1, 13.4 years for zone 2, 17.3 years for zone 3, and 13.3 years for zone 4, which indicates zone 2 and zone 4 are very less active compared to zone 1 and zone 3 for M=5.8 (Figure 7).

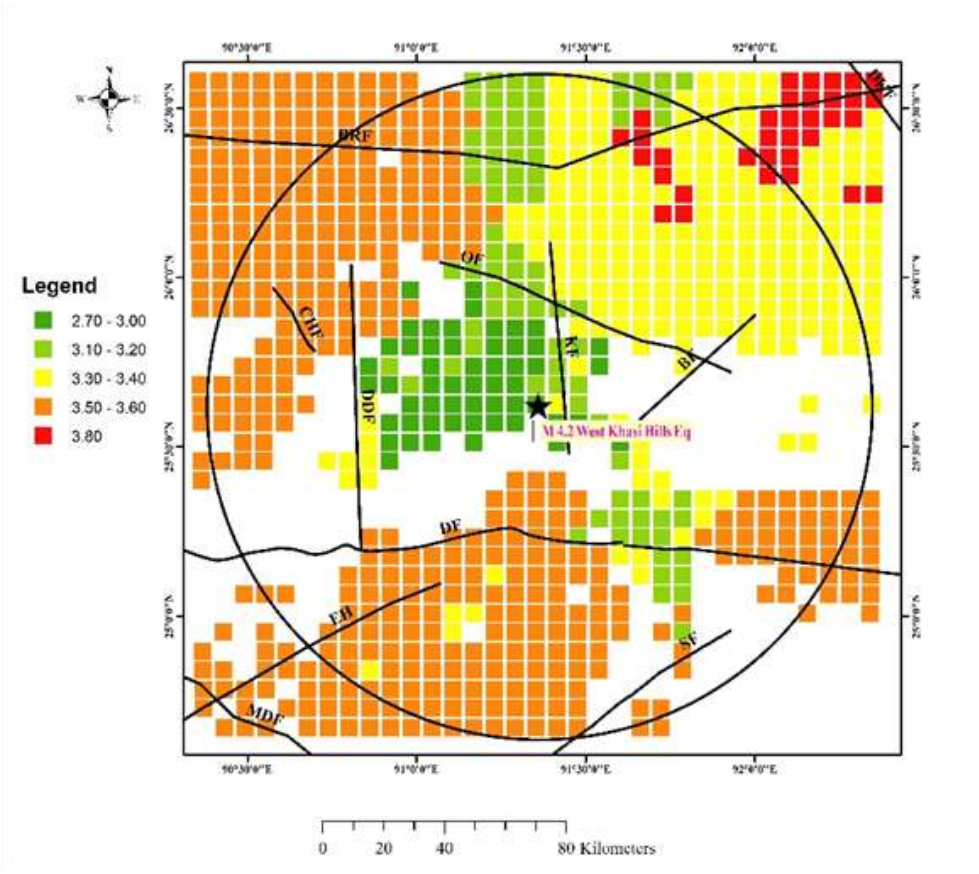

Fig. 5 Spatial distribution of the magnitude of completeness (M_C).

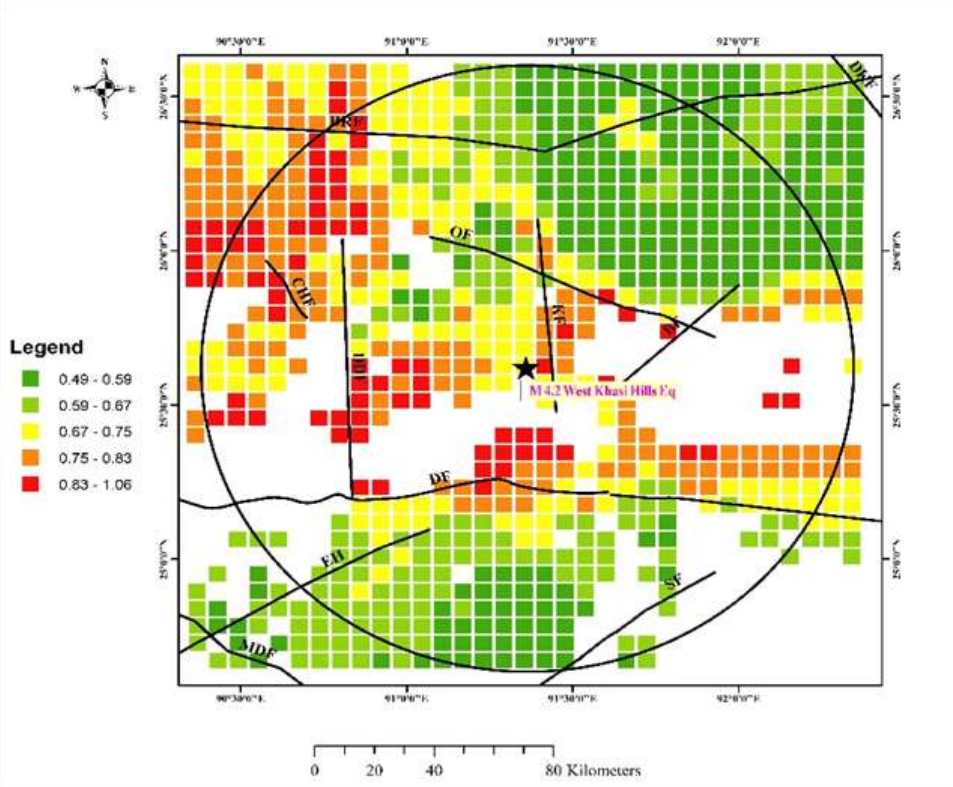

Fig. 6 Spatial distribution of the b-values.

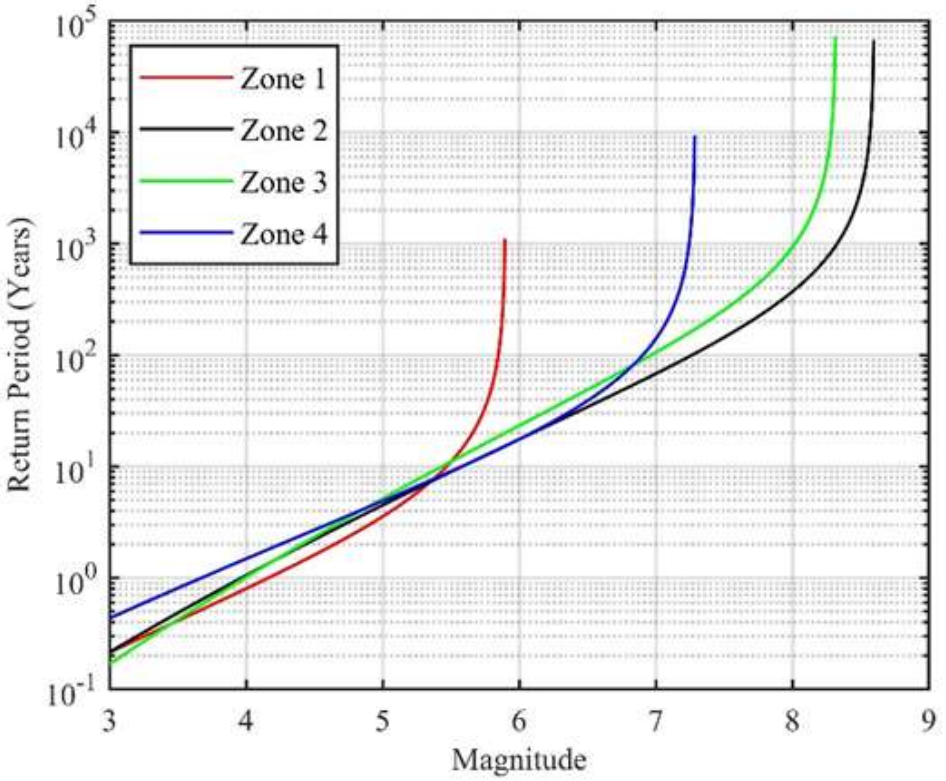

Fig. 7 Return period vs magnitude for delineated 4 zones.

The Bouguer gravity anomaly over the SP varies from – 90 mGal on the northern side to + 50 mGal on the southern side (Figure 4). The local disturbances of the Bouguer anomaly can be seen across some major faults on the Bouguer anomaly map (Figure 4). A smaller variation can be observed across the southerly dipping reverse Brahmaputra reverse fault. The Bouguer anomaly variation across the sinistral slip Barapani Shear Zone is observed due to the transition from high-grade metamorphic rocks to a low-grade meta-sedimentary unit, so-called the Shillong Group. Similarly, variation from negative to positive Bouguer anomaly can be identified towards the west of our study area, where a recent earthquake has been observed near the Kulsi fault. Large disturbances in the Bouguer anomaly can be observed towards the southern side of the Shillong Plateau, possibly due to the presence of some highly dense material as well as the presence of north-dipping, steep reverse Dauki fault, which marks the southern Boundary of the Shillong Plateau. The two reverse faults that are dipping towards each other, the Brahmaputra reverse fault and the Dauki fault, mark the boundary of the Shillong Plateau, along which the plateau has been uplifted and formed the most enigmatic tectonic feature, also called the pop-up structure, in northeast India. Some faults have low b-values around them, suggesting areas with high earthquake vulnerability.

CONCLUSIONS

In the present study, the following key observations have been made:

- The mean magnitude of completeness (M_C) for the compiled earthquake catalogue is 3.0, with a spatial distribution ranging from 2.7 to 3.8.
- The mean b-value and a-value for the entire study area are 0.62 ± 0.04 and 4.8, respectively.
- The spatial variation plot reveals a significantly low b-value in the epicentral region of the West Khasi Hills earthquake compared to the surrounding areas, indicating a region of tectonic stress accumulation.
- Lower b-values are also observed in regions to the northeast and south of the epicenter, suggesting that these areas may be prone to future earthquakes.
- The return periods of an earthquake M=5.8 are 52.5 years for zone 1, 13.4 years for zone 2, 17.3 years for zone 3, and 13.3 years for zone 4.
- The variation of the Bouguer gravity anomaly map demarcates major faults within the study region, identifying the earthquake-prone zone between the Shillong Plateau and the Brahmaputra Valley.

These findings provide valuable insights that can be used for seismic hazard estimation in the region.

REFERENCES

1. Aki, K. (1965). “Maximum Likelihood Estimate of b in the Formula log N= a-bM and its Confidence limits”, *Bull Earthq Res Inst, Tokyo Univ,* Vol. 43, pp. 237–239.
2. Bhattacharya, P.M., Majumdar, R.K. and Kayal, J.R. (2002). “Fractal dimension and b-value mapping in northeast India”, *Curr Sci*, Vol. 82, pp. 1486–1491.
3. BIS (2002). “IS 1893–2002 (Part 1): Indian standard Criteria for Earthquake Resistant Design of Structures, Part 1–general Provisions and Buildings”.
4. Bora, D.K., Borah, K., Mahanta, R. and Borgohain, J.M. (2018). “Seismic B-Values and its Correlation with Seismic Moment and Bouguer Gravity Anomaly over Indo-Burma Ranges of Northeast India: Tectonic Implications. Tectonophysics”, Vol. 728–729, pp. 130–141. https://doi.org/10.1016/j.tecto.2018.01.001
5. Bora, D.K., Borah, K., Singh, A.P. and Mishra, O.P. (2022). “Distribution of B-Values in Indo-Burma Ranges, Northeast India: Implications to Structural Heterogeneities and Style of Faulting”, *Geol J*, Vol. 57, pp. 5284–5293. https://doi.org/10.1002/gj.4294
6. Borgohain, H., Baruah, S. and Sarmah, R.K. (2018a). “An Appraisal on Recent Trend of Seismicity in Shillong Plateau with Special Emphasis to Plateau Pop-Up”, *Int J basic Appl Res,* Vol. 8, pp. 1218–1229.

7. Borgohain, J.M., Borah, K., Biswas, R. and Bora, D.K. (2018b). "Seismic B-Value Anomalies Prior to the 3rd January 2016, Mw = 6.7 Manipur Earthquake of Northeast India", *J Asian Earth Sci*, Vol. 154, pp. 42–48. https://doi.org/10.1016/J.JSEAES.2017.12.013
8. Choy, G.L. and Boatwright, J.L. (1995). "Global Patterns of Radiated Seismic Energy and Apparent Stress", *J Geophys Res*, Vol. 100, No. 18205–18228. https://doi.org/10.1029/95jb01969
9. CNDM (2002). "Scenario of Seismic Hazard in Assam", *In: Cent. Nat. Assam Adm. Staff Off. Disaster Manag.* http://aasc.nic.in/course material/Disaster/scenario of seismic hazard in assam.pdf. Accessed 12 Dec 2019
10. Copley, A., Avouac, J-P. and Royer, J-Y. (2010). "India-Asia Collision and the Cenozoic slowdown of the Indian Plate: Implications for the Forces Driving Plate Motions", *J. Geophys. Res. Solid Earth*, pp. 115.
11. Cornell, BYCA (1968). "Engineering seismic risk analysis", *Bull Seismol Soc Am*, Vol. 58, pp. 1583–1606.
12. Hanks, T.C. and Kanamori, H. (1979). "A Moment Magnitude Scale", *J Geophys Res*, Vol. 84, pp. 2348–2350.
13. Hirt, C., Yang, M., Kuhn, M., Bucha, B., Kurzmann, A. and Pail, R. (2019). "SRTM2gravity: An Ultrahigh Resolution Global Model of Gravimetric Terrain Corrections", *Geophysical Research Letters*, Vol. 46, pp. 4618–4627. https://doi.org/10.1029/2019GL082521
14. Iyengar, R.N., Sharma, D. and Siddiqui, J.M. (1999). "Earthquake History of India in Medieval Times", *Indian J Hist Sci*, Vol. 34, pp. 181–238.
15. Kanamori, H. (1983). "Magnitude Scale and Quantification of Earthquakes", *Tectonophysics*, Vol. 93, pp. 185–199. https://doi.org/10.1016/0040-1951(83)90273-1
16. Khan, P.K. (2005). "Mapping of B-Value Beneath the Shillong Plateau", *Gondwana Res*, Vol. 8, pp. 271–276. https://doi.org/10.1016/S1342-937X(05)71126-6
17. Khan, P.K., Ghosh, M., Chakraborty, P.P. and Mukherjee, D. (2011). "Seismic b-Value and the Assessment of Ambient Stress in Northeast India", *Pure Appl Geophys*, Vol. 168, pp. 1693–1706. https://doi.org/10.1007/s00024-010-0194-x
18. Kijko, A. (2004). "Estimation of the maximum earthquake magnitude, mmax", *Pure Appl Geophys*, Vol. 161, pp. 1655–1681. https://doi.org/10.1007/s00024-004-2531-4
19. Kumar, A., Kotoky, N. and Shekhar, S. (2024). "Spatial Variation of Seismicity Parameters in Meghalaya, North-East India", *Acta Geophys*. https://doi.org/10.1007/s11600-024-01290-x
20. Kumar, M.R., Raju, P.S., Devi, E.U., Saul, J. and Ramesh, D.S., 2004. "Crustal Structure Variations in Northeast India from Converted Phases", *Geophys Res Lett*, pp. 31. https://doi.org/https://doi.org/10.1029/2004GL020576
21. Lay, T. and Wallace, T.C. (1995). "Modern Global Seismology".
22. Nayak, G.K., Rao, V.K., Rambabu, H.V. and Kayal, J.R. 2008. "Pop-Up Tectonics of the Shillong Plateau in the Great 1897 Earthquake (Ms 8.7): Insights from the Gravity in Conjunction with the Recent Seismological Results", *Tectonics*, pp. 27. https://doi.org/10.1029/2006TC002027
23. Oldham, R.D. (1899). "Report on Great Earthquake of 12th June 1897", *Mem Geol Sur India*, Vol. 29, pp. 1–39.
24. Oldham, T. (1882). "The Cachar earthquake of 10th January 1869".
25. Pandey, A.K., Chingtham, P. and Prajapati, S.K., et al. (2019). "Recent Seismicity Rate Forecast for North East India: An Approach Based on Rate State Friction Law", *J Asian Earth Sci*, Vol. 174, pp. 167–176. https://doi.org/10.1016/j.jseaes.2018.12.004
26. Pandey, A.K., Chingtham, P. and Roy, P.N.S. (2017). "Homogeneous Earthquake Catalogue for Northeast Region of India using Robust Statistical Approaches", *Geomatics, Nat Hazards Risk*, Vol. 8, pp. 1477–1491. https://doi.org/10.1080/19475705.2017.1345794
27. Rajendran, C.P., Rajendran, K. and Duarah, B.P., et al. (2004). "Interpreting the Style of Faulting and Paleoseismicity Associated with the 1897 Shillong, Northeast India, Earthquake: Implications for Regional Tectonism", *Tectonics*, Vol. 23, pp. 1–12. https://doi.org/10.1029/2003TC001605

28. Richter, C.F. (1935). "An Instrumental Earthquake Magnitude Scale", *J Geol*, Vol. 25, pp. 1–32. https://doi.org/10.1086/622062
29. Sarkar, P., Mondal, S., Pal, S.K., Roy, P.N.S., Sahoo, S.D., Widyadwatmaja, A., Gupta, S. and Gupta, A. (2022). "New Insights on the Tectonic Framework using EIGEN6C4 Gravity Data, Seismicity, and Finite Element Stress Analysis: An Attempt to Map Earthquake Vulnerable Zones in Parts of North-East India and Surroundings", *Physics and Chemistry of the Earth*, pp. 127. https://doi.org/10.1016/j.pce.2022.103195
30. Scholz, C.H. (1968). "The Frequency-Magnitude Relation of Microfracturing in Rock and its Relation to Earthquakes", *Bull Seismol Soc Am*, Vol. 58, pp. 399–415.
31. Schorlemmer, D., Neri, G., Wiemer, S. and Mostaccio, A. (2003). "Stability and Significance Tests for B-Value Anomalies: Example from the Tyrrhenian Sea", *Geophys Res Lett*, Vol. 30, pp. 1–4. https://doi.org/10.1029/2003GL017335
32. Shahabuddin, M. and Mohanty, W.K. (2025). "An Updated and Unified Complete Earthquake Catalogue of the Shillong Plataea and Adjoining Region", *Seismol Res Lett*, Vol. 20, pp. 1–22. https://doi.org/10.1785/0220240217
33. Sharma, V. and Biswas, R. (2022). "Spatio-Temporal Variation in B-Value Prior to the 26 November 2021 Mizoram Earthquake of Northeast India", *Geol J*, Vol. 57, pp. 5361–5373. https://doi.org/10.1002/gj.4635
34. Sharma, V. and Biswas, R. (2024). "Seismic Hazard Assessment and Source Zone Delineation in Northeast India: A Case Study of the Kopili Fault Region and Its Vicinity", *Indian Geotech J*, Vol. 54, pp. 598–626. https://doi.org/10.1007/s40098-023-00792-7
35. Sharma, V., Bora, D.K. and Biswas, R. (2022). "Spatio-Temporal Analysis of B-Value Prior to 28 April 2021 Assam Earthquake and Implications Thereof", *Ann Geophys*, pp. 65, pp. 1–15. https://doi.org/10.4401/ag-8802
36. Shi, Y. and Bolt, B.A. (1982). "The Standard Error of the Magnitude-Frequency b Value", *Bull Seismol Soc Am*, Vol. 72, pp. 1677–1687.
37. Thingbaijam, K.K.S., Nath, S.K. and Yadav, A., et al. (2008). "Recent Seismicity in Northeast India and its Adjoining Region", *J Seismol*, Vol. 12, pp. 107–123. https://doi.org/10.1007/s10950-007-9074-y
38. Urbancic, T.I., Trifu, C.I., Long, J.M. and Young, R.P. (1992). "Space-Time Correlations of b Values with Stress Release", *Pure Appl Geophys PAGEOPH*, Vol. 139, pp. 449–462. https://doi.org/10.1007/BF00879946
39. Utsu, T. (1965). "A Method for Determining the Value of b in Formula log n= a-b*M Showing the Magnitude-Frequency for Earthquakes (with English Summary)", *Geophys Bull Hokkaido Univ*, Vol. 13, pp. 99–103.
40. Verma, R.K. and Mukhopadhyay, M. 1977a. "An Analysis of the Gravity Field in Northeastern India".
41. Wiemer, S. (2001). "A Software Package to Analyze Seismicity: ZMAP", *Seismol Res Lett*, Vol. 72, pp. 373–382. https://doi.org/10.1785/gssrl.72.3.373
42. Wiemer, S. and Wyss, M. (2000). "Minimum Magnitude of Completeness in Earthquake Catalogs: Examples from Alaska, the Western United States, and Japan", *Bull Seismol Soc Am*, Vol. 90, pp. 859–869. https://doi.org/10.1785/0119990114
43. Woessner, J. and Wiemer, S. (2005). "Assessing the Quality of Earthquake Catalogues: Estimating the Magnitude of Completeness and its Uncertainty", *Bull Seismol Soc Am*, Vol. 95, pp. 684–698. https://doi.org/10.1785/0120040007
44. Wyss, M. (1973). "Towards a Physical Understanding of the Earthquake Frequency Distribution", *Geophys J R Astron Soc*, Vol. 31, pp. 341–359. https://doi.org/10.1111/j.1365-246X.1973.tb06506.x
45. Wyss, M., Shimazaki, K. and Wiemer, S. (1997). "Mapping Active Magma Chambers by b Values Beneath the Off-Ito Volcano", *Japan.pdf. J Geophys Res*, Vol. 102, pp. 20413–20422. https://doi.org/10.1029/97JB01074

46. Yadav, R.B.S., Bormann, P. and Rastogi, B.K., et al. (2009). "A Homogeneous and Complete Earthquake Catalog for Northeast India and the Adjoining Region", *Seismol Res Lett*, Vol. 80, pp. 609–627. https://doi.org/10.1785/gssrl.80.4.609
47. Yadav, R.B.S., Chauhan, P. and Sandhu, M., et al (2023). "Spatial Distribution of the Gutenberg-Richter Parameters and Fractal Dimension and Their Correlations in Northeast India and Its Vicinity", *In: Proceedings of 17th Symposium on Earthquake Engineering*, pp 137–150.